Future Broadband Packet Radio Access and Its Field Experiments

Mamoru Sawahashi, Hiroyuki Atarashi, and Kenichi Higuchi

IP Radio Network Development Department, NTT DoCoMo, Inc.
3-5 Hikari-no-oka Yokosuka-shi, Kanagawa-Ken, 239-8536 Japan

***Abstract* - This paper presents a broadband packet radio access scheme based on Orthogonal Frequency Division Multiplexing (OFDM) based access in the downlink and single-carrier based access with spreading including low-rate channel coding in the uplink for the systems beyond IMT-2000. In our design concept for radio access in both links, the spreading factor including the channel coding rate is optimally controlled so that the system capacity is maximized according to the cell configuration, i.e., whether cellular cell or local environments, by taking advantage of one-cell frequency reuse, and orthogonality of simultaneous users in the frequency domain is used. We show that peak throughput values of greater than 100 Mbps and 20 Mbps are achieved using variable spreading factor (VSF)-Orthogonal Frequency and Code Division Multiplexing and broadband DS-CDMA access in a real field environment using the implemented base station and mobile station transceivers employing 100-MHz bandwidth in the downlink. Furthermore, we present results of a real-time 1-Gbps packet transmission with the corresponding frequency efficiency of 10 bits/second/Hz in the downlink employing VSF-Spread OFDM radio access utilizing 4-by-4 multiple-input multiple-output multiplexing.**

I. INTRODUCTION

The evolution of UMTS Radio Access (UTRA) and the UMTS Radio Access Network (UTRAN) was proposed and approved at the 3GPP Plenary Meeting last December. It is anticipated that the evolved form of UTRA will adopt shared-channel-based packet access employing Orthogonal Frequency Division Multiplexing (OFDM) based radio access, which is robust against multipath interference (MPI) in a wider channel bandwidth than the current 5-MHz bandwidth. Furthermore, the evolved forms of UTRA and UTRAN will be designed to enable a short delay (i.e., low latency) and have affinity to IP-based core networks, in order to provide rich high-rate services at low cost. Following the proposal of the evolved forms of UTRA and UTRAN in the 3GPP, research on future broadband packet radio access (i.e., the systems beyond IMT-2000) will be accelerated to achieve packet-based rich multimedia mobile communications offering high-resolution video, streaming, and high-speed data download services.

This paper presents a broadband packet radio access scheme based on OFDM based access in the downlink and single-carrier based access with spreading including low-rate channel coding in the uplink for the systems beyond IMT-2000 [1]. In our design concept of radio access in both links, the spreading factor (*SF*) including the channel coding rate is optimally controlled so that the system capacity is maximized according to the cell configuration, i.e., whether cellular cell or local environments, by taking advantage of one-cell frequency reuse, and orthogonality of simultaneous users in the frequency domain is used in addition to that in the time domain. First, Section II presents the proposed broadband radio access schemes. In Section III, we present the field experimental results from the implemented testbed based on variable spreading factor (VSF)-orthogonal frquency and code division multiplexing (OFCDM), to show that throughput exceeding 100 Mbps in the downlink is achieved. Furthermore, in Section IV, we present a real-time 1-Gbps packet transmission with the corresponding frequency efficiency of 10 bits/second/Hz in the downlink VSF-Spread OFDM access scheme utilizing 4-by-4 multiple-input multiple-output (MIMO) multiplexing.

II. BROADBAND PACKET RADIO ACCESS CANDIDATE

The use of an all packet-based radio access network (RAN) and an air interface is desirable considering the affinity to full IP-based core networks. All traffic including real-time traffic with a strict delay requirement is conveyed by the packet switching mode. Moreover, further reduction in the network cost is a very important requirement in order to offer rich multimedia services to customers via wireless communications. A higher system capacity, i.e., higher frequency efficiency accommodating a large sector throughput, will definitely contribute to further reduction in the RAN cost.

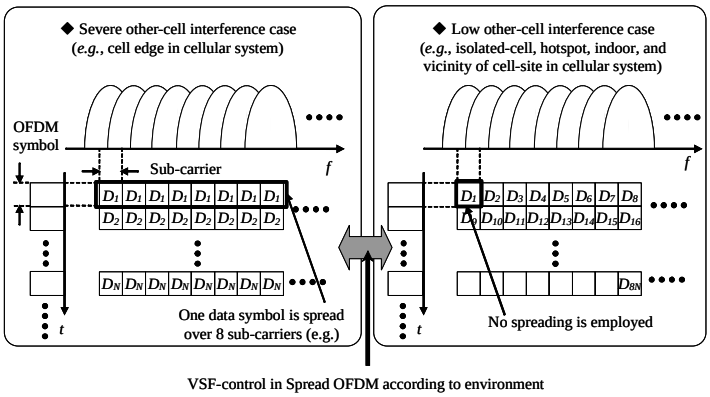

Figure 1. Proposed Variable Spreading Factor (VSF)-control scheme

2.1 Downlink Radio Access: VSF (Variable Spreading Factor)-Spread OFDM

In order to mitigate the increasing level of MPI, OFDM based radio access is very promising owing to its inherent immunity to MPI associated with a low symbol rate using many sub-carriers together with the insertion of a guard interval. Furthermore, OFDM has a high affinity to advanced techniques, such as frequency domain channel-dependent scheduling, MIMO multiplexing/diversity, and enhanced multicast/broadcast transmission.

In future radio access systems, various deployment scenarios are envisaged such as wide area environments for a cellular system with a multi-cell configuration and a local area environment such as isolated-cell, very-small-cell (hotspot), and indoor environments. Our proposed concept for a radio access scheme is to support both wide and local area environments using the same air interference by only changing the radio parameters. To enable this design concept, we propose applying variable spreading factor (VSF)-control [2] to OFDM with spreading (Spread OFDM).

Figure 1 shows the principle of VSF-Spread OFDM. In the proposed VSF Spread-OFDM, we apply frequency domain channel-dependent scheduling (i.e., frequency chunk assignment to the optimum user based on the link conditions) or frequency diversity by using interleaving and spreading over the entire channel bandwidth [3],[4] based on one-cell frequency reuse. Thus, the entire channel bandwidth is basically used in all the cells. In cellular environments with a multi-cell configuration, one-cell frequency reuse is essential to increase the system capacity. In the proposed VSF-control scheme, when inter-cell interference from the surrounding cells is severe, such as at the cell-boundary in a cellular environment, spreading and very-low-late channel coding (as a part of spreading) is employed. Accordingly, the processing gain associated with the spreading gain and channel coding gain suppresses inter-cell interference, although at a sacrifice of the achievable data rate. Note that, in this case, in order to obtain the spreading gain, code-multiplexing is not used except for some special cases.

Meanwhile, under low inter-cell interference conditions such as in an isolated cell, hotspot, indoors, or in the immediate vicinity of a cell-site in a cellular environment, spreading and very-low-rate channel coding are not employed to achieve the maximum data rate (capacity)

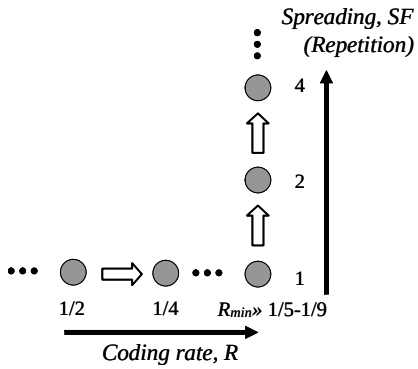

Figure 2. Combination of very low-rate channel coding and spreading

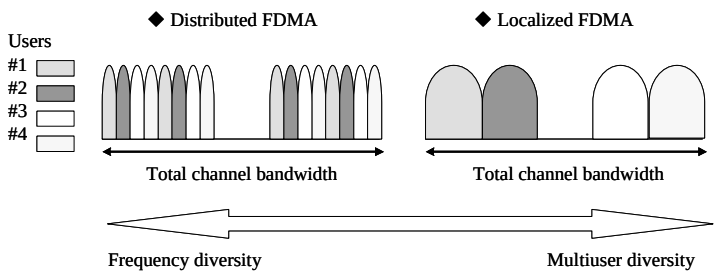

Figure 3. Distributed FDMA and localized FDMA

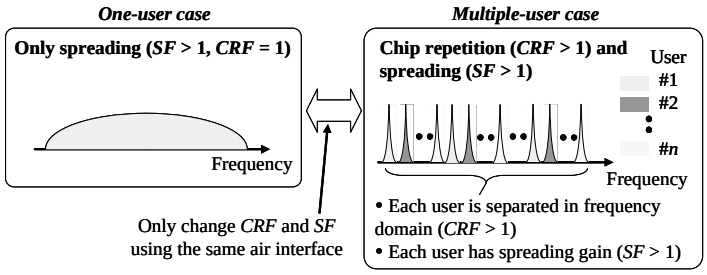

Figure 4. VSCRF-CDMA radio access scheme in uplink

under the respective interference conditions. Therefore, based on the VSF-control, seamless support of various radio environments becomes possible through the continuous use of the same radio access by adaptively controlling the coding rate and *SF* according to inter-cell interference depending on the deployment scenario, propagation channel conditions, etc. Consequently, we aim to achieve the maximum system capacity in the respective cell configurations and radio channel conditions using the same air interface, thereby, the same broadband radio access scheme with the same air interface (i.e., the same carrier frequency, frequency bandwidth, and radio frame format). It was clarified in [5] that the channel coding should be used as a part of spreading with priority rather than simple spreading, i.e., repetition coding, with a random sequence, because an additional channel coding gain is obtained. The improvement in the channel coding gain is reduced according to the decrease in the coding rate. Therefore, in the proposed VSF-control scheme, a combination of low-rate channel coding with the minimum coding rate of approximately R_{min} = 1/5-1/9 and simple spreading with the spreading factor of *SF* is employed, when a larger processing gain beyond 1/ R_{min} is necessary as shown in Fig. 2.

In the OFDM based packet radio access, channel-dependent packet scheduling using both the time and frequency domains is very effective in improving the sector and user throughput. In the two-dimensional channel-dependent scheduling, the optimum transmission unit (or chunk) proving a high received signal -to-interference plus noise power ratio (SINR) is assigned to each user, bringing about a diversity effect among simultaneous accessing users. When the amount of traffic is greater than the payload size in one frequency block, i.e., chunk, one or a few chunks are assigned to one user exclusively. When multiplexing the data streams of low-rate users in the same chunk of the same transmission time interval (TTI), time division multiplexing (TDM) (symbol-symbol), frequency division multiplexing (FDM), or a hybrid of TDM and FDM (two-dimensional mapping) is used. Furthermore, code division multiplexing (CDM) is advantageous for multiplexing low-rate channels with almost a constant rate such as the control signal channel, in which QPSK modulation is employed. In this case, CDM obtains a large frequency diversity effect associated with the transmission using the entire channel bandwidth, which exceeds the degradation due to inter-code interference.

2.2 Uplink Radio Access: Single-Carrier Based Radio Access

In the uplink, power-efficient transmission is necessary considering the restriction to the transmission power of the user equipment (UE) terminal unlike the situation in the downlink. Single-carrier radio access provides an inherent lower peak-to-average power ratio (PAPR) than multi-carrier based radio access such as orthogonal frquency division multiple access (OFDMA). This feature is very advantageous for enabling low power consumption of the UE terminal. Therefore, focusing on providing wide coverage in cellular system rather than the achievable peak data rate near the cell site, single-carrier based radio access seems more promising than the OFDMA access scheme.

The "gain" for suppressing inter-cell interference is necessary for achieving one-cell frequency reuse. Therefore, we first reduce the channel coding rate, because the channel coding gain is more effective than the spreading gain [5]. In addition, we use spreading (repetition) when further processing gain is required similar to downlink . Therefore, spreading is used only to suppress the inter-cell interference and residual intra-cell and multipath interference.

The application of orthogonality between simultaneously accessing users in the frequency in addition to the time domains is very beneficial in mitigating the intra-cell interference, which leads to improvement in the system capacity and the achievable data rate. There are two types of orthogonality in the frequency domain, Localized FDMA and Distributed FDMA (comb-shaped spectrum) as shown in Fig. 3. Among these two, the localized FDMA is a conventional FDMA using a pre-assigned transmission bandwidth. Furthermore, as the excellent realization of distributed FDMA, IFDMA was proposed, which achieves orthogonality of simultaneously accessing users employing a comb-shaped spectrum [6]. In IFDMA, by coherently accumulating comb-shaped components that are uniquely assigned to each user, an effect equivalent to despreading, i.e., interference suppression, is obtained. When the same comb-shaped component sets are used in the adjacent cell, nevertheless, more severe co-channel interference occurs assuming one-cell frequency reuse. Therefore, we proposed adaptively controlling the *SF* and chip repetition factor (*CRF*) according to various radio conditions, the cell structure, and the number of accessing users, which was proposed as variable spreading and chip repetition factor (VSCRF)-CDMA as shown in Fig. 4 [7]. When the inter-cell interference is large in cellular environments, we use spreading in addition to the use of a very-low channel coding rate. However, we do not use spreading along with a high coding rate particularly in local areas, where the inter-cell interference is small. When there are multiple accessing uses in the same frequency block, we increase the chip repetition factor value so that orthogonality among users is achieved. In a single-user case, we do not use chip repetition. In single-carrier access, the influence of a delayed path is large unlike in OFDMA access. Thus, employing an equalizer or multipath interference canceller (MPIC) is essential to improve the peak data rate under multipath fading conditions. In particular, simplified equalization in the frequency domain by the use of a cyclic prefix at every Fast Fourier Transform (FFT) processing block is feasible.

III. FIELD EXPERIMENT ON PROPOSED BROADBAND RADIO ACCESS

3.1 Configuration of Implemented Base Station and Mobile Station Transceiver

The major radio link parameters of the implemented base station (BS) and mobile station (MS) transceivers are given in Table I [8]. We applied VSF-OFCDM with a 101.5-MHz bandwidth and 768 sub-carriers in the downlink. VSF-OFCDM employs a total *SF* (= SF_{Time} x SF_{Freq}) of greater than one in a multi-cell environment to achieve higher link

Table I. Major Radio Link Parameters of Testbed

		Downlink	Uplink
Carrier frequency		4.635 GHz	4.900 GHz
Bandwidth		101. 5 MHz	40 MHz
Number of sub-carriers		768 (131.836 kHz sub-carrier separation)	2
Symbol duration		7.585 *m*sec + GI 1.674 *m*sec (1024 + 226 samples)	–
Chip rate		–	16.384 Mcps / carrier
Spreading factor		SF_{Time} x SF_{Freq} = 16 x 1, C_{mux} = 15	SF = 4, C_{mux} = 1, 2, 3
Modulation	Data	QPSK, 16QAM, 64QAM	QPSK
	Spreading	QPSK	Hybrid PSK
Channel coding		Turbo code (R = 1/3, 1/2, 3/4)	Turbo code (R = 1/3, 1/2)

capacity by establishing one-cell frequency reuse along with the use of a cell-specific scrambling code. In two-dimensional spreading, we prioritize time domain spreading rather than frequency domain spreading. This is because, in a frequency selective fading channel, time domain spreading is generally superior to frequency domain spreading in maintaining the orthogonality among the code-multiplexed channels. Thus, the link performance of the VSF-OFCDM is almost identical to that of VSF-Spread OFDM, since the orthogonality among multiplexing codes is maintained. In the uplink, in order to demonstrate the achievable peak throughput of one user, we do not employ the chip repetition function of VSCRF-CDMA, since there is no need to suppress multiple access interference (MAI). Therefore, we investigate broadband CDMA with a 40-MHz bandwidth with two sub-carriers in the uplink, in which the optimized sub-carrier bandwidth is employed based on the tradeoff between the improvement in the Rake time diversity effect and the degradation due to increasing MPI.

The configurations of the BS and MS are shown in Figs. 5 (a) and 5(b), respectively. In the BS transmitter, the binary information bit is first turbo encoded with the rate of R = 1/3 and the constraint length of four bits. In order to generate the rates of R = 1/2 and 3/4, the output of the parity bits from the turbo encoder of R = 1/3 is punctured. After data modulation mapping, symbol interleaving in the frequency domain is performed within every OFCDM symbol to randomize the burst errors due to frequency-selective fading. The interleaved sequence is transmitted by the downlink shared data channel, which is spread by SF_{Time} x SF_{Freq} = 16 x 1 and then, C_{mux} = 15 code channels are multiplexed. In the downlink shared data channel, adaptive modulation and channel coding (AMC) based on the measured SINR is applied. The downlink shared control channel is used to convey the modulation and channel coding scheme (MCS) information in the AMC. Furthermore, the pilot symbols used for channel estimation and SINR measurement for the AMC are time-multiplexed into the downlink shared data channel and downlink shared control channel. After conversion into baseband in-phase (I) and quadrature (Q) components by a D/A converter, quadrature-modulation is performed. Finally, the IF modulated signal is up-converted into the RF signal and amplified by the power amplifier, where the center carrier frequency is 4.635 GHz. At the BS receiver, the frequency down-converted IF signal is first linearly amplified by an automatic gain control (AGC). The received spread signal is converted into the baseband I and Q components by a quadrature detector. The resultant signals are converted into digital format by an A/D converter and filtered by a square-root raised cosine Nyquist filter. We generate a power delay profile in order to search the propagation paths for Rake combining. The composite signal sample sequence is despread by a matched filter and Rake-combined by using a channel estimate. Finally, the soft-decision data sequence from the coherent Rake combiner is turbo-decoded to recover the transmitted data sequence. Max-Log-MAP decoding with eight iterations is used as the decoding algorithm.

At the MS transmitter, the binary information bit sequence in the uplink shared data channel is channel-encoded using turbo coding. After the coded bit sequence is serial-to-parallel converted into C_{mux} code channels, the data sequence of each code channel is QPSK data-modulated. Subsequently, the data modulated sequence is spread by the combination of the orthogonal variable spreading factor (OVSF) channelization code with a SF = 4-chip length and a scrambling code with the repetition period of 8,192 chips. After the pilot channel comprising 32 symbols with SF = 256 is code-multiplexed into a coded data channel, a square-root raised cosine Nyquist transmit filter is applied at each sub-carrier. Then, the D/A converted baseband I and Q components are quadrature-modulated, and the IF modulated signal is up-converted into an RF carrier frequency. At the MS receiver, we apply two-branch antenna diversity reception. The channel gain of each frame at each sub-carrier is estimated by coherently accumulating pilot symbols within a frame. By employing the channel estimate, the spread sequence at each sub-carrier is despread in the time domain with Equal Gain Combining and in the frequency domain with Minimum Mean Square Error combining. After de-interleaving in the frequency domain, turbo decoding is performed to recover the information bit sequence. Meanwhile, the measured received SINR information at the MS for selecting the optimum MCS is sent to the BS.

3.2 Field Experimental Results

Field experiments in an actual multipath fading channel are conducted in the urban area of Yokosuka city nearby Tokyo. The heights of the BS and MS antennas are approximately 50 m and 3 m from the ground, respectively. A measurement vehicle equipped with a MS is driven along the measurement course at the average speed of approximately 30 km/h, where the distance from the BS is approximately 800 m at Points A and B, and approximately 1000 m at Points C and D. Furthermore, most of the measurement course is under non-line-of-sight conditions due to residential apartment buildings and office buildings between the BS and MS, except for the middle point between Points C and D.

A. Measured propagation channel characteristics

Figures 6(a) and 6(b) show examples of the measured instantaneous power delay profile and the corresponding measured instantaneous received signal level of each sub-carrier in the frequency domain over 101.5 MHz at Point X in Course A-B, respectively. As shown in Fig. 6(a), many delayed multipath components are distributed over the duration of approximately 2 *m*sec, where the measured root mean squared (r.m.s.) delay spread becomes approximately 0.35 *m*sec. The measured

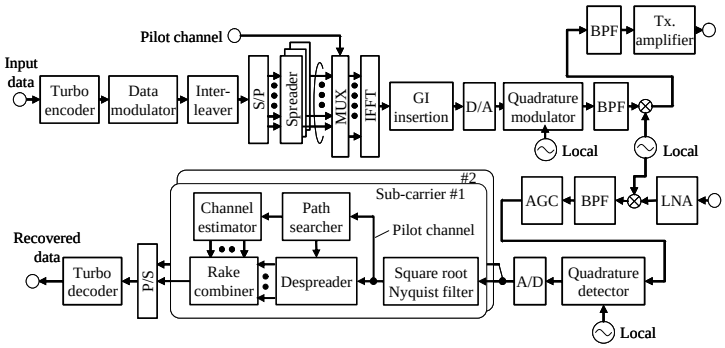

(a) Base station

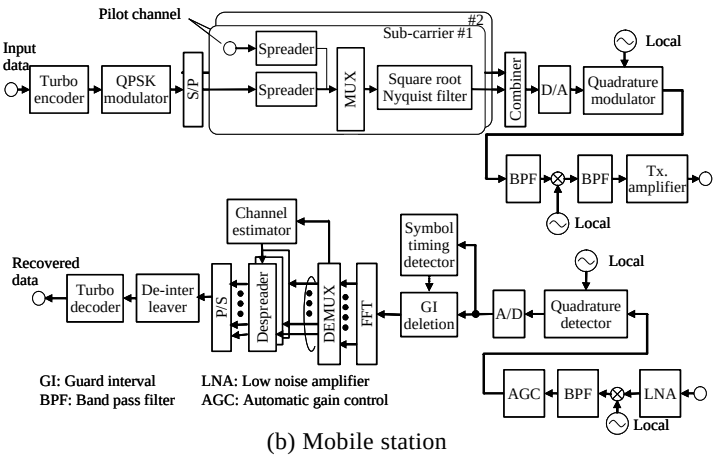

(b) Mobile station

Figure 5. Configuration of implemented transceiver

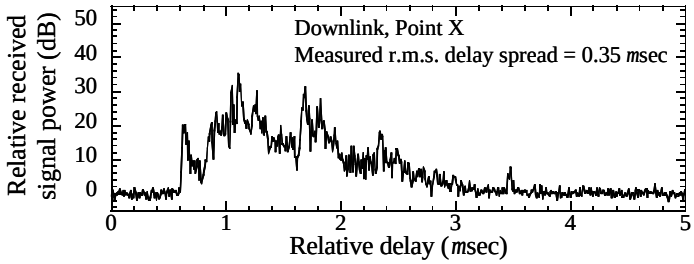

(a) Measured instantaneous power delay profile

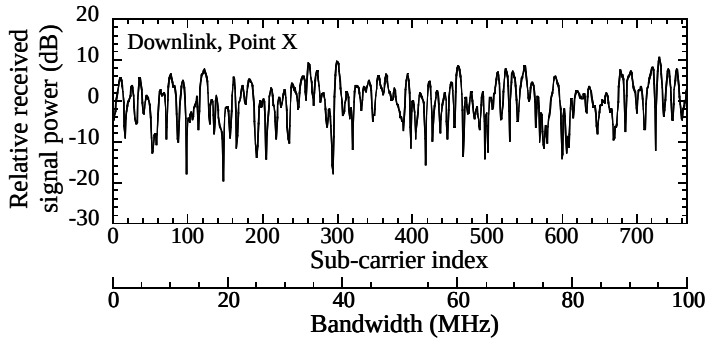

(b) Measured channel variation in frequency domain

Figure 6. Measured propagation channel

power delay profile is approximated by the exponentially decayed model. Moreover, Fig. 6(b) shows that the received signal level of each sub-carrier varies with a wide range of nearly 30 dB, resulting in a severe frequency-selective fading channel.

Figure 7 shows the cumulative distribution of the measured received SINR averaged over 100-msec per receiver antenna of the respective courses and the aggregate course in the downlink when the BS transmission power is 10W. In the average received SINR measured by using the pilot symbols, the interference plus noise power includes the interference power caused by the delayed multipath, which exceeds the guard interval duration, and the thermal noise power at the MS receiver. It is clear that the measured average received SINR in Course D-A becomes lower than those in the other courses due to the obstruction caused by tall buildings between the BS and the course. On the other hand, in Course C-D containing line-of-sight locations, the location probability with the average received SINR of greater than 20 dB is approximately 30%. Consequently, we find that the location probabilities with the average received SINR of greater than 6, 10, and 15 dB in the aggregate course (A-B-C-D-A) are approximately 90, 65, and 20%, respectively.

B. Throughput performance

The measured throughput performance in the VSF-OFCDM downlink when AMC with six MCSs, i.e., MCS1 (QPSK, R = 1/3), MCS2 (QPSK, R = 1/2), MCS3 (QPSK, R = 3/4), MCS4 (16QAM, R = 1/2), MCS5 (16QAM, R = 3/4), and MCS6 (64QAM, R = 3/4), is applied is plotted in Fig. 8 as a function of the average received SINR per antenna over the entire course. The measured throughput performance of each MCS is also given for comparison. Figure 8 shows that the higher the average received SINR is, the more efficient MCS is selected, indicating that AMC achieves an increase in the instantaneous throughput using adaptive rate control under real propagation channel conditions. Furthermore, we find that the throughput values of 100, 200, and 300 Mbps are achieved at the average received SINR of approximately 6.0, 14.0, and 20.0 dB, respectively, associated with AMC operation with antenna diversity reception. As a result, from the cumulative distribution of the measured average received SINR in Fig. 7, the throughput values of 100 and 200 Mbps are achieved at the location probability of approximately 90 and 20%, respectively, in the course. Therefore, these results show that throughput over 100 Mbps employing OFCDM radio access with a 100-MHz bandwidth is possible in cellular

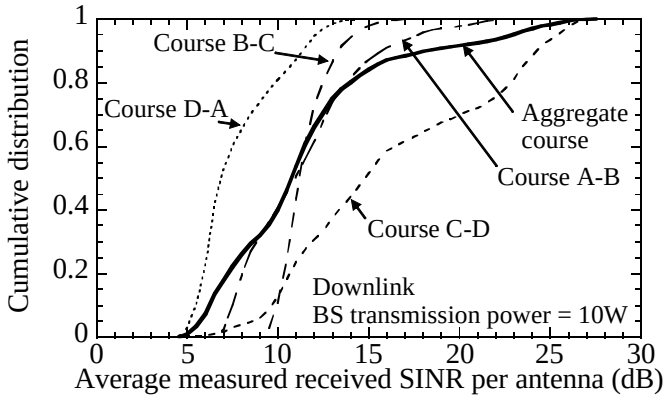

Figure 7. Cumulative distribution of average measured received SINR

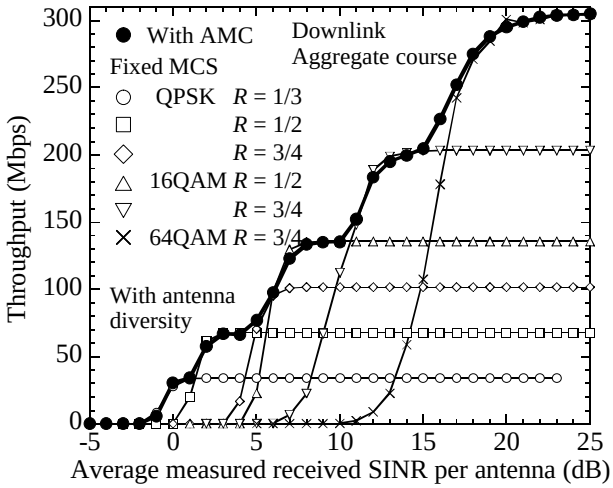

Figure 8. Measured throughput performance of each MCS and AMC in downlink

environments where the distance between the BS and MS is approximately 1000 m at maximum at the average moving speed of approximately 30 km/h.

IV. 1-GBPS DATA TRANSMISSION EMPLOYING MIMO TECHNIQUE FOR SHORT-DISTANCE AREA WITH HIGH TRAFFIC

It is anticipated that a much higher data rate than 100 Mbps is necessary particularly in local areas where an extremely large amount of traffic is concentrated in a limited short coverage area. Therefore, in our concept, the achievable peak throughput in these areas is approximately 1 Gbps (i.e., frequency efficiency of 10 bits/second/Hz) assuming limited conditions such as short-distance areas with a short time dispersion, employing the identical air interface parameters such as frequency bandwidth, carrier frequency, duplexing, radio access, and frame structure. Under such limited channel conditions with a short time dispersion in a short coverage area, utilization of MIMO multiplexing is promising [9, 10, 11]. Among decoding schemes, nevertheless, the maximum likelihood detection (MLD) can reduce the required signal energy per-bit-noise power spectrum density ratio (E_b/N_0) satisfying the required average bit error rate or packet error rate better than can the Vertical-Bell Laboratories layered Space Time (V-BLAST) [12] or the Minimum Mean Squared Error (MMSE) methods. Thus, from the viewpoint of the achievable throughput increase derived through MIMO multiplexing, the MLD approach is the most promising. As is well known, however, the computational complexity level in MLD is increased exponentially according to the increase in the modulation level in the data modulation scheme and the number of transmitter antenna branches. Then, a promising approach that applies QR decomposition associated with the M-algorithm to MLD (hereafter

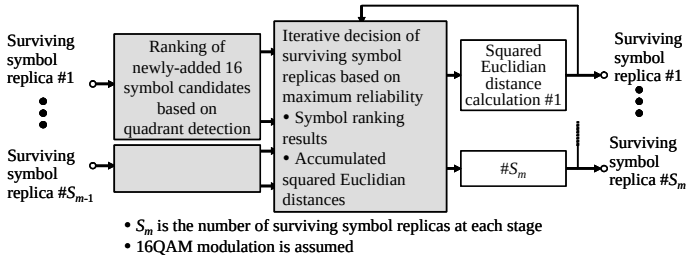

Figure 9. Proposed adaptive selection algorithm for surviving symbol replica candidates based on maximum reliability

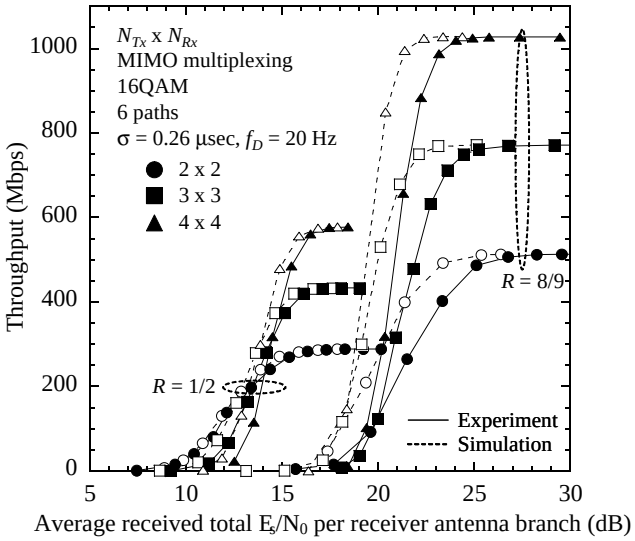

Figure 10. Measured throughput performance with transmitter/ receiver antenna branches as a parameter

QRM-MLD) was proposed in [13], leading to a remarkable reduction in the computational complexity level compared to that of conventional MLD for OFDM MIMO multiplexing. Furthermore, we recently proposed an adaptive selection algorithm for surviving symbol replica candidates based on the maximum reliability (hereafter ASESS) in QRM-MLD for OFDM MIMO multiplexing [14]. In the original QRM-MLD method in [13], the branch metric, i.e., squared Euclidian distance, is calculated for all additional symbol replica candidates at each stage corresponding to each surviving symbol replica from the previous stage. Thus, our idea is to calculate the branch metric only for the additional symbol replica candidates with high reliability, which are selected with priority by symbol ranking based on multiple quadrant detection. The branch metric is then calculated only for those symbol replica candidates using an iterative loop in descending order of the accumulated branch metric from the symbol replica with the maximum accumulated branch metric, i.e., minimum accumulated squared Euclidian distances (See Fig. 9).

We implemented real-time 1-Gbps packet transmission transceiver in VSF-Spread OFDM radio access using MIMO multiplexing with the maximum of four transmitter/receiver branches. Then, we investigated the measured throughput performance at the number of transmitter/receiver branches as a parameter using the implemented MIMO multiplexing transceiver in the laboratory experiments. In the experiments, we employed 16 multipath fading simulators to simulate frequency-selective Rayleigh fading channels. A six-path channel is generated using multipath fading simulators, where each path is independently Rayleigh-faded with the r.m.s. delay spread, s, of 0.26 μsec and the fading maximum Doppler frequency of 20 Hz. Figure 10 indicates the measured throughput of the QRM-MLD with the ASESS when the combination of (N_{Tx}, N_{Rx}) is changed from two to four as a function of the average received total E_b/N_0 per receiver branch. Here, the total E_b denotes the signal energy per bit of total transmission signal of N_{Tx} antenna branches, since we assume a constant total transmission power irrespective of the N_{Tx} value for fair comparison. When the N_{Tx} value is two, three, and four, the information bit rate becomes 289, 433, and 578 Mbps and 514, 771, and 1028 Mbps for the coding rate of R = 1/2 and 8/9, respectively. We find from the figures when the average received total E_b/N_0 is less than approximately 14 dB, the obtained throughput becomes lower according to an increase in the N_{Tx} and N_{Rx} values due to the degradation in the signal detection. Figure 14 shows, however, that when the average received total E_b/N_0 is greater than approximately 14 dB, where the influence of additive noise is small, the measured throughput is increased according to the increase in the combination of (N_{Tx}, N_{Rx}). The throughput values of approximately 400 Mbps, 700 Mbps, and 1 Gbps are achieved by 2-by-2, 3-by-3, and 4-by-4 MIMO multiplexing, respectively, at the average received E_b/N_0 of 23.5 dB for 16QAM modulation with R = 8/9. In conclusion, we demonstrated real-time extremely high-speed packet transmission of greater than 1 Gbps in the implemented MIMO OFDM transceivers.

V. CONCLUSION

This paper presented a broadband packet radio access scheme based on OFDM based access in the downlink and single-carrier based access with spreading including low-rate channel coding in the uplink for the systems beyond IMT-2000. In our design concept of radio access in both links, the *SF* including the channel coding rate is optimally controlled so that the system capacity is maximized according to the cell configuration, i.e., whether cellular cell or local environments, by taking advantage of one-cell frequency reuse, and orthogonality of simultaneous users in the frequency domain is used. We showed that peak throughput values of greater than 100 Mbps was achieved using VSF-OFCDM radio access in a real field environment using the implemented BS and MS transceivers employing 100-MHz bandwidth in the downlink. Furthermore, we presented the results of a real-time 1-Gbps packet transmission with the corresponding frequency efficiency of 10 bits/second/Hz in the downlink employing VSF-Spread OFDM access applying four-by-four MIMO multiplexing together with 16QAM data modulation and punctured turbo coding.

REFERENCES

[1] H. Atarashi, S. Abeta, and M. Sawahashi, "Broadband packet wireless access appropriate for high-speed and high-capacity throughput," in Proc. IEEE VTC2001-Spring, pp. 566-570, May 2001.

[2] H. Atarashi, S. Abeta, and M. Sawahashi, "Variable spreading factor orthogonal frequency and code division multiplexing (VSF-OFCDM) for broadband packet wireless access," IEICE Trans. Commun., vol. E86-B, no. 1, pp. 291-299, Jan. 2003.

[3] N. Yee, J.-P. Linnartz, and G. Fettweis, "Multi-carrier CDMA in indoor wireless radio networks," in Proc. IEEE PIMRC'93, pp. 109-113, Sept. 1993.

[4] K. Fazel and L. Papke, "On the performance of convolutional-coded CDMA/OFDM for mobile communication systems," in Proc. IEEE PIMRC'93, pp. 468-472, Sept. 1993.

[5] A.J. Viterbi, CDMA: Principles of spread spectrum communication, Addison-Wesley 1995

[6] M. Schnell, I. Broeck, and U. Sorger, "A promising new wideband multiple-access scheme for future mobile communication," European Trans. on Telecommun. (ETT), vol. 10, no. 4, pp. 417-427, July/Aug. 1999.

[7] Y. Goto, T. Kawamura, H. Atarashi, and M. Sawahashi, "Variable Spreading and Chip Repetition Factors (VSCRF)-CDMA in reverse link for broadband wireless access," in Proc. IEEE PIMRC2003, pp. 254-259, Sept. 2003.

[8] Y. Kishiyama, N. Maeda, K. Higuchi, H. Atarashi, and M. Sawahashi, "Field experiments on throughput performance over 100 Mbps in forward link for VSF-OFCDM broadband radio access," IEICE Trans. on Commun., vol. E88-B, no. 2, pp.604-614, Feb. 2005.

[9] G. J. Foschini, Jr., "Layered space-time architecture for wireless communication in a fading environment when using multi-element antennas," Bell Labs Tech. J., pp. 41-59, Autumn 1996.

[10] R. D. Murch and K. B. Letaief, "Antenna Systems for Broadband Wireless Access," IEEE Commun. Mag., vol. 40, no. 4, pp. 76-83, April 2002.

[11] A. van Zelst, R. van Nee, and G. A. Awater, "Space division multiplexing (SDM) for OFDM systems," in Proc. IEEE VTC2000-Spring, pp. 1070-1074, May 2000.

[12] P. W. Wolniansky, G. J. Foschini, G. D. Golden, and R. A. Valenzuela, "V-BLAST: an architecture for realizing very high data rates over the rich-scattering wireless channel," in Proc. 1998 URSI International Symposium on Signals, Systems, and Electronics, pp. 295-300, Sep. 1998.

[13] K. J. Kim and J. Yue, "Joint channel estimation and data detection algorithms for MIMO-OFDM systems," in Proc. Thirty-Sixth Asilomar Conference on Signals, Systems and Computers, pp. 1857-1861, Nov. 2002.

[14] K. Higuchi, H. Kawai, N. Maeda, and M. Sawahashi, "Adaptive selection of surviving symbol replica candidates based on maximum reliability in QRM-MLD for OFCDM MIMO multiplexing," in Proc. IEEE Globecom2004.